Journal of the Nigerian Association of Mathematical Physics
Volume27, (July, 2014), pp241 – 250
© J. of NAMP

Surface Energy and Surface Relaxation of the (0001) Surface of HCP metals Using the Analytical Equivalent Crystal Theory

E. Aghemenloh[1], I. S. Okunzuwa[2], S. Yusuf[3]

[1,2]Department of Physics, University of Benin, Benin City, P.M.B. 1154, Edo State, Nigeria.
[3]Department of Science Laboratory, Kogi State Polytechnic, Lokoja, Kogi State, Nigeria

Abstract

The analytical equivalent crystal theory of Zypman and Ferrante which is a modification of the ECT have been used to establish a data base of surface energy for the (0001) surface of 10 hcp metals such as Be, Mg, Sc, Ti, Y, Zr, Tc, Ru, Hf and Re. The effect of relaxation on the computed surface energy values have been found to be of the order of 4 – 10% from Be to Re. The surface energies obtained are in good agreement with experiment and other theoretical values.

Keywords:hcp metals, AECT, Surface energy, (0001) surface

1.0 Introduction

It is now well established that metal surfaces undergo relaxation [1]. The experimental results are mainly obtained by low - energy electron diffraction (LEEDS) [1,2] which, if the measurements are analyzed by multiple – scattering calculations, enables the determination of the atomic positions at the surface [2]. These studies have demonstrated that the outermost atomic layer of most clean metal surfaces shows an inward relaxation; that is, that the spacing between the top two layers is smaller than the bulk interlayer spacing. The top – layer relaxation is often accompanied by smaller shifts of the second and third layers, which can be directed either inward or outward. As a general rule, the magnitude of the relaxation is larger for rough surfaces than for smooth ones, and in many cases a reconstruction of the surface is also observed.

Early theoretical efforts for describing the phenomenon of relaxation started with the self – consistent jellium model of Lang and Kohn [3], followed by the electrostatic model of Finnis and Heine [4], based on a smoothing of the electron charge density parallel to the surface. Allan and Lannoo [5] presented a tight – binding calculation that indicated the inward displacement of the surface layer observed, with few exceptions, experimentally. The damped oscillatory character of multilayer relaxation was predicted later by Barnett et al. [6, 7], who included the evaluation of the screening response of the conduction electrons to the relaxed ionic system. Later, Jiang et al. [8] developed an empirical version of the point ion model which provides good agreement with experimental results for Fe and Al. However, the predictive power of this model is limited by the need of a parameter adjusted to experimental relaxations. Other theoretical works include the total energy calculations of Ho and Bohnen [9], Fu et al. [10], Eguiluz [11], Davenport and Weinert [12], Hamann and Feibelman [13, 14] and Methfessel et al. [15].

The experimental determination of structures of clean surfaces is quite extensive [16]. But, while the body of experimental work grows, first – principles theoretical calculations are more limited because of the computational difficulties for cases of low symmetry. Thus, in the last decades, there has been a trend to complement these costly calculations by simple, semi - empirical methods, which properly describe the energetic of defects in metals. Two such methods, the embedded atom method (EAM) [17], based on density functional theory, and equivalent crystal theory (ECT) [16, 18 – 20], based on perturbation theory have been extensively used to that effect. Both methods have been applied to the study of surface relaxation [16, 18-20, 21-24].

Surface energy and surface relaxation of fcc and bcc materials [16, 18-20] have been calculated using the original equivalent crystal theory method (ECT) developed by Smith and co-workers [18-20]. Recently, an extension of the ECT was introduced by Zypman and Ferrante [25]. The analytical equivalent crystal theory (AECT) which has been shown to increase the computational speed of the ECT has also been extensively used to describe the energetic of defects in metals [26, 27].

Corresponding author: E. AghemenlohE-mail:aeusibius6@gmail.com,Tel.: +2348033611224

However, it has not been applied to calculate surface relaxation in metals. Our aim therefore, is to present the first AECT surface relaxation and surface energy of the top layers of the (0001) surface of hcp metals. In this work, we ignore parallel relaxation as well as surface reconstruction and dealt only with rigid perpendicular translation of the near surface planes.

This paper is structure as follows. In section 2, we give a brief discussion of the analytical equivalent crystal theory method (AECT). In section 3, we discuss the AECT method of calculating the surface relaxation and surface energies of hcp metals. The results of surface energies and relaxations for 10 hcp metals are reported in section 4, along with the results obtained by other workers. Section 5, summarizes our main conclusions.

2.0 The analytical ECT method

In ECT the total energy of a collection of atoms near a defect is the sum of individual energy contributions $U(a_{eq})$, where a_{eq} is called an equivalent lattice parameter and $U(a_{eq})$, is explicitly given by the Universal binding energy relation (UBER) [17] which is simply parameterized in terms of physically known constants in the Rydberg function. In ECT an atom near a defect is viewed as sensing a reduced or increased electron density. This condition is then interpreted as a point on the UBER in terms of an expanded or contracted perfect crystal. Perturbation theory is used to obtain the equivalent lattice parameter of the expanded or contracted crystal, a_{eq} in terms of a_0 the lattice parameter corresponding to the perfect crystal. Once a_{eq} is known, the energy of the atom near the defect is obtained from that point on the UBER. The value of a_{eq} is obtained in terms of a_0 from the inversion of the basic ECT transcendental equation. Although conceptually simple, the inversion process represents the computational time consuming step in the implementation of the algorithm.

The implementation of ECT involves a perturbation equation that determines the energy of a solid with a defect in terms of a perfect crystal of the same substance expanded or contracted from the equilibrium lattice parameter to a new “equivalent” lattice parameter. This procedure is equivalent to finding an embedding electron density ρ. A typical atom at a given location is embedded in a density ρ produced by the electronic charge density of the remainder atoms in the system. The yet unknown, equivalent nearest-neighbour distance, R_{eq} satisfies

$$N_1 R_{eq}^p \exp(\alpha R_{eq}) + N_2 (c_2 R_{eq})^p \exp[-(\alpha + 1/\lambda)]c_2 R_{eq}] \quad = \quad \rho \qquad (1)$$

where N_1, is the number of nearest neighbours in the equivalent crystal, N_2 is the number of next-nearest neighbours, c_2 is the ratio of the next-nearest-neighbour distance to the nearest-neighbour distance, and α, p and λ are known material-dependent constant. In many applications of ECT to evaluate defect formation energies, ρ on the right-hand side of Eq. (1), is written in a form similar to the left-hand side. For example, the density produced by neighbours on an atom next to a vacancy is

$$\rho = N_1^1 R_0^p \exp(-\alpha R_0) + N_2^1 \left(c_2 R_{eq}\right)^p \exp[-(\alpha + 1/\lambda) c_2 R_0],$$

where $N_1^1 = N_1 - 1$ and $N_2^1 = N_2$ because the atom in question loses one nearest-neighbour (where the vacancy is located) but loses no second nearest neighbour. In this example, the lattice is unrelaxed and consequently R_0 represents the nearest neighbour distance of the perfect crystal. This shows explicitly that R_{eq} is the unknown in Eq. (1). Once R_{eq} is obtained, ECT uses this value in the UBER function, $U(a_{eq})$. The corresponding energy cost is then $U(a_{eq}) - U(a_o)$. In what follows, we adopt the method of Zypman and Ferrante [25].

The general problem is therefore to find the function

$$R_{eq} = G(\rho) \qquad (2)$$

Eq. (1) can be cast in dimensionless form by defining

$$y \equiv \alpha R_{eq}$$

$$y^p \exp(-y) + \frac{N_2}{N_1} c_2^p y^p \exp[-(1 + 1/\alpha\lambda) c_2 y] \; = \; \frac{\rho \alpha^p}{N_1} \qquad (3)$$

By introducing $\left(1 + \frac{1}{\alpha\lambda}\right) c_2 - 1 \equiv \gamma$, $\frac{N_2}{N_1} \equiv n_{21}$, $\frac{\rho \alpha^p}{N_1} \equiv x$, Eq. (3) becomes

$$y^p \exp(-y)\left(1 + n_{21} c_2^p y^p \exp(-\gamma y)\right) = x \qquad (4)$$

The constant αλ is about unity and $c_2 > 1$, thus $\gamma > 0$, which is a conservative lower bound for γ. By using appropriate values from Table 1, one finds that $n_{21}c_2^p y^p e^{-\gamma y} < 0.08$ in Table 2. Thus, in Eq. (4), the second term inside the parenthesis is much smaller than unity, and therefore it is dropped in many real applications. Thus, the problem reduces to finding the roots of

$$y^p \exp(-y) = x \qquad (5)$$

A sketch of Eq. (5) is shown in Fig.1. In Fig.1, the root y_1 corresponds to the smaller lattice parameter while the root y_2 corresponds to the larger lattice parameter. Creating a vacancy effectively lowers the atom density thereby increasing y [20]. Thus the physically accepted root is y_2.

Eq. (5) can now be recast in the Lambert form:

$$(\frac{-y}{p})\exp(\frac{-y}{p}) = \frac{-x^{\frac{1}{p}}}{p} \qquad (6)$$

with the solution

$$y = -pW_{-1}(\frac{-x^{\frac{1}{p}}}{p}) \qquad (7)$$

where W_{-1} is the Lambert function [29, 30]. The sub index "-1" labels the branches. The Lambert function has an infinite number of complex branches with only two purely real, the branches known as "0" and "-1".

Define (y_M, x_M) as the point corresponding to the maximum attainable density, as indicated in Fig.1. y_M may be found by setting $\left[\frac{dx}{dy}\right]_{Y=Y_M}$ to zero from Eq.(4) thus

$$p - y_M + n_{21}c_2^p \exp(-\gamma y_M)\left[p-(1+\gamma)y_M\right] = 0 \qquad (8)$$

Next, γ_m and y_{Mm} are obtained as defined in Ref. [25]. The procedure for obtaining them is asfollows. Eq. (8) cannot be solved analytically for y_M, but it can be solved for γ as

$$\gamma \equiv \Omega^{-1}(y_M) = \frac{1}{y_M}\left[p - y_M - w_0\left(\frac{-(p-y_M)\exp(p-y_M)}{n_{21}c_2^p}\right)\right] \qquad (9)$$

y_{Mm} can then be found from Eq. (9) be setting $\frac{1}{\left(\frac{d\Omega^{-1}(y_M)}{dy_M}\right)_{y_M=y_{Mm}}} = 0$, hence,

$$(p - y_{Mm})y_{Mm}^2\left[1 + W_0\left(\frac{(y_{Mm}-p)\exp(p-y_{Mm})}{n_{21}c_2^p}\right)\right] = 0 \qquad (10)$$

The only non-trivial solution to Eq. (10) is for the argument of the Zero branch to be -1/e. For a complete discussion of equations (8) to (10), the interested reader is referred to the work of Zypman and Ferrante [25], where the details can be found. According to Zypman and Ferrante, the smallest possible value of $y(= y_{\min})$ is given as

$$y_{\min} = p - W_0(n_{21}\frac{c_2^p}{e}) \qquad (11)$$

Eq.(11) was used to evaluate the $y_{\min}$ in Table 2.

3.0 Surface energy calculation

3.1 Rigid surface

In this section, we implement the analytical algorithm by Zypman and Ferrante for the ECT. The surface energy and surface relaxation of the (0001) plane of 10 hcp metals are obtained by this algorithm. Consider a rigid surface where no interlayer relaxation is allowed. Therefore, all

Bond lengths and angles retain their bulk equilibrium values. Thus $F^*[a_2^*] = F^*[a_3^*] = F^*[a_4^*]$ $= 0$. The surface energy is therefore obtained by solving for the 'volume' term represented by $F^*[a_1^*]$ only. Even with the above simplification, the calculation of the surface energy of hcp metals, within the ECT method, unlike the bcc and fcc metals, is not straight forward. This is mainly due to the fact that the 12 nearest-neighbour atoms of the hcp structure are not all at the same distance. Six of them are at a distance R_{nn1}, while the other six are at a slightly different distance R_{nn2}.

In this study we have adopted the convention that the smaller distance will always be denoted as R_{nn1}. If a and c are the lattice constants for the hcp metals, then for all the hcp metals considered in this study, $R_{nn1} = [(4a^2 + 3c^2)/12]^{1/2}$, and $R_{nn2} = a$, for the ideal hcp ratio of $\sqrt{8/3}$. For hcp structure, 6 atoms are at the next nearest-neighbour distance $R_{nnn} = [(16a^2 + 3c^2)/12]^{1/2}$. In Ref. [35], the surface energy calculations for the hcp metals were organised into three theoretical models of interest because of the complexity of the hcp structure. Here, we neglect models II and III of Ref. [35] and concentrated on model I, the true ECT model. Results from this model using analytical ECT will be compared with other theoretical results and experiments.

In order to obtain the density ρ of the (0001) plane, we notice that a typical surface atom has lost 3 nearest neighbours (out of 12 for an atom in the bulk) and 3 next nearest neighbours (out of 6 for a bulk atom). Hence,

$$\rho = 3R_{nn1}^p \exp(-\alpha R_{nn1}) + 6R_{nn2}^p \exp(-\alpha R_{nn2}) + 3R_{nnn}^p \exp[-(\alpha + 1/\lambda)R_{nnn}] \tag{16}$$

Solving Eq. (16), we obtain the value of the electron density ρ.
Next, we solve for x from the relation

$$x = \frac{\rho\alpha^p}{12} \tag{17}$$

and then using the ProductLog function in Mathematica, we get

$$y = -p\,\mathrm{Pr}oduct\,Log\left[-1, \frac{-x^{\frac{1}{p}}}{p}\right] \tag{18}$$

Now, after obtaining the value of x from Eq. (17), we then compute the nearest neighbour distance R_{eq} from the relation

$$R_{eq} = \frac{y}{\alpha} \tag{19}$$

Once the value of y has been obtained from Eq.(18) and knowing the value of the material constant α, we can then calculate the value of R_{eq} from Eq. (19). Next, we compute the lattice parameter $a_{eq}$from

$$a_{eq} = c_2 R_{eq} \tag{20}$$

where $c_2 = R_{nnn}/R_{nn1.}$

Once the values of R_{eq} are known from Eq. (19), then the values of a^* and F^* can be calculated directly [20]. The surface energy σ_{001} is then calculated from the formula [35]

$$\sigma_{001} = \frac{2\Delta E}{a^2\sqrt{3}} \sum_j F^*\left[a_1^*, (j)\right] \tag{21}$$

The sum over j includes only one atom per atomic layer and usually only a few layers need be included for metal low index planes. In fact, for the (001) hcp metal surface, only the outer most surface layer is involved.

3.2 Relaxed Surface

Now, let consider the simplest surface relaxation, that is, a rigid displacement of the top surface layer towards the bulk. Then, the contribution from the higher order anisotropic terms must be included. The assumption here is that only the surface plane is allowed to relax, and only perpendicular relaxation was considered. Letting the planes close to the surface relax turns on the other three contributions to the energy. Some bonds are compressed, contributing to $F^*[a_2^*]$, the bond angles near the surface as well as the difference between face diagonal are distorted, generating an increase of energy via $F^*[a_3^*]$ and $F^*[a_4^*]$. Also, allowing the atoms in the surface region to relax introduces the additional complexity of including in the calculation more non-equivalent atoms, located in deeper layers. Many-atom effects, which are represented in the ECT by the inclusion of the three atom bond-angle anisotropy and the four-atom face diagonal distortion terms [16,20,36] are necessary, but in the case of surface energy calculations of metals, of very little relevance. As have been shown in other previous ECT works [16, 20, 36], they introduce a small correction, usually of the order of 1 to 2% of the leading term (Eq. (2) of Ref. [20]. Therefore, the last two terms of the ECT expansion have been neglected in this study. This is however not the case for semiconductors, where angular anisotropies are a significant contribution to the surface energy.

In this work, we concentrated on the perpendicular relaxation of the top layer (d_{12}) surface of the (0001) face of hcp metals, ignoring parallel relaxation as well as surface reconstruction. Although some of these surfaces are known to reconstruct, we did not look for this effect in our calculations. Figure 2 shows the (0001) planes of hcp metals and the different contribution of each plane after the creation of the surface. The reference atom i is on the surface plane j = 1, with the neighbour atoms in each plane. Let assume that the top plane (j = 1) is slightly contracted by a distance z towards the first plane below the surface (j = 2), but the plane j = 2 as well as any other plane below, are at their normal bulk positions. The rigid interplanar spacing is $d = c/2$ (c is one of the equilibrium lattice parameters of the hcp metal); therefore, the distance between the plane j = 1 and j = 2 is $c/2 - z$. Following the notation of Fig. 2, the AECT equations for the atoms in these planes are:

$$\rho = 6a^p \exp(-\alpha a) + 3r\, r_z^p \exp(-\alpha z) + 3 r_a^p \exp[-(\alpha + 1/\lambda) r_a] \qquad (j=1) \tag{22}$$

$$\begin{aligned}\rho = {} & 6a^p \exp(-\alpha a) + 3r_{nn1}^p \exp(-\alpha r_{nn1}) + 3r_z^p \exp(-\alpha r_z) \\ & + 3r_{a_1}^p \exp[-(\alpha + 1/\lambda) r_{a_1}] + 3s_o^p \exp[-(\alpha + 1/\lambda) s_o] \qquad (j=2)\end{aligned} \tag{23}$$

where

$$r_{z_2} = [\frac{a^2}{3} + \frac{c^2}{4} + c^2 z^2 - c^2 z]^{1/2} \tag{24}$$

$$r_a = [\frac{4a^2}{3} + \frac{c^2}{4} + c^2 z^2 - c^2 z]^{1/2} \tag{25}$$

and

$$s_0 = r_{nnn} = [(16a^2 + 3c^2)/12]^{1/2} \tag{26}$$

Eqs. (22) and (23) are then solved for each value of z to obtain the value of electron density ρ, in order to determine the corresponding equivalent crystal nearest neighbour distance R_{eq}.

The volume contribution to the surface energy is therefore given by

$$\sigma_1 = \frac{\Delta E}{A} \sum_{j=1}^{2} F^*(a_{1,j}^*(z)) \tag{27}$$

where

$$a_{1,j}^* = (\frac{R_{eq}^j}{c_1} - r_{WSE})/l \tag{28}$$

c_1 is the ratio between the nearest neighbour distance and r_{WSE} is the undistorted actual crystal and $r_{WSE} = (3\sqrt{3}a^2 c/16\pi)^{1/3}$.

Next, the bond compression contributions to the surface energy for the atoms in the planes j = 1 and 2 are computed. The AECT equations associated with this defect are:

$$\rho = 12R_0^p \exp(-\alpha R_0) - 6A_2 R_0^p (r_z - R_0)\exp[-\beta(r_z - R_0)] = 0 \ (j = 1) \tag{29}$$

$$\rho = 12R_0^p \exp(-\alpha R_0) - 3A_2 R_0^p (r_z - R_0)\exp[-\beta(r_z - R_0)] = 0 \ (j = 2) \tag{30}$$

where

$$A_2 = \frac{D}{6\sqrt{2}ac}$$

and the quantity D is given by

$$D = N_1 \exp(-\alpha R_0)(\alpha R_0 - p)$$

Again, Eqs. (29) and (30) are solved for ρ in order to obtain R_{eq}. The energy contribution is then given by

$$\sigma_2 = \frac{\Delta E}{A}\sum_{j=1}^{2} F^*(a_{2,j}^*(z)) \tag{31}$$

Summarizing, the surface energy of hcp (0001) face, where only the top layer is allowed to relax, is given by

$$\sigma_{0001} = \frac{\Delta E}{A}[\sum_{j=1}^{2} F^*(a_{1,j}^*(z)) + \sum_{j=1}^{2} F^*(a_{2,j}^*(z))] \tag{32}$$

4. Results and Discussion

In this section we exhibit the results obtained in this study. First, the input data needed for the calculations and the ECT constants l, p, α, λ and r_{WSE} computed with the help of the input data are exhibited in Table 1. We have carried out an extensive calculation of surface energies of relaxed (but unreconstructed) (0001) surface for some selected hcp metals. Although some of these metals are known to reconstruct, we did not look for this effect in our calculations with the sole purpose of generating a large data set of surface energy values from which patterns can be extracted. The equivalent crystal nearest-neighbour distance is a very vital parameter in the ECT method, since it is the parameter needed in the calculation of surface energy. The AECT results of the unrelaxed and relaxed surface energies for 10 hcp metals are presented in Table 3. It can be seen from the table that the values of the unrelaxed (rigid) surface energies are larger than the relaxed values. The decrease in surface energy values due to the effect of relaxation is of the order of 4 - 10% as we move from Be to Re. This is clearly shown in Fig.3. It is evidence from the table also that the contribution of surface energies from the electron density change effect (volume term) of the ECT is much greater than the bond-compression term, thus justifying the neglect of the other many-body terms usually associated with the ECT method [16,36].

The results of surface energies obtained by different workers for 10 hcp metals are presented in Table 4. The Table contains theoretical results [37, 38, 39-42] and experimental results [43].The theoretical methods include, modified embedded atom method (MEAM) [39, 40], analytical modified embedded atom method (AMEAM) [41], empirical electron theory (EET) [42], and first-principles calculation [37, 38]. The experimental values are determined from measurements of the surface tension of liquid metals extrapolated through a liquid-solid phase transition. From Table 4, it can be seen that our relaxed AECT surface energy results are in good agreement with experiment and first-principles calculations. Our results for 3d, 4d, and 5d metals differ from reported experimental values by about 29% and from first-principles values by about 18%. However, it must be pointed out that experimental measurements of the surface energy are more commonly found for polycrystalline materials. Figure 4 shows a plot of our surface energy results compared with first-principles values [37], semi-empirical values [39] and experimental values [43]. The figure exhibits the typical parabolic dependence on the d occupation which is already well known [15, 37], and in accord with the simple picture of d-electron contribution to surface energy suggested by Friedel [44]. For the semi-empirical models whose results are presented in Table 4, with the exception of Refs. [39, 40] our surface energy results are uniformly larger and closer to experiment and first-principles calculations except for Hf and Tc where Ref. [42] predict otherwise. AECT results are also in reasonable agreement with the results of Baskes and Johnson [39].However, it should be noted that our surface energy results listed in Table 4 are for the relaxed surface as compared to the other theoretical works in the same table where relaxation effect were not taken into account. Notwithstanding, our present AECT results still compare well with other theoretical and experimental values. Hence, for a consistent comparison of our AECT surface energies with ab initio and other semi-empirical theoretical calculations, the effect of surface relaxation commonly ignored in surface energy studies should be included in future work.

Table 1: Pure metal properties: Lattice constants a and c, and cohesive energy ΔE are from Ref. [29], Bulk modulus B are from Refs. [29,30] and experimental monovacancy formation energies E_{1V}^{f} for Mg, Ti, Zr,and Zn are from Ref. [30], while E_{1V}^{f} for other metals are assumed to beapproximately 1/3 of cohesive energy [30-32].

Element	ΔE(eV)	$E_{1v}^{f}(eV)$	a(Å)	c(Å)	B($10^{11}\,Jm^{-3}$)	p	l (Å)	λ (Å)	α(Å^{-1})	r_{WSE}(Å)
Be	3.32	1.11	2.27	3.59	1.144	2	0.315	0.886	1.576	1.241
Mg	1.52	0.80	3.21	5.21	0.369	4	0.313	0.881	1.694	1.771
Sc	3.90	1.30	3.31	5.27	0.435	6	0.458	1.288	2.247	1.814
Ti	4.85	1.55	2.95	4.68	1.097	6	0.341	0.959	2.712	1.615
Y	4.37	1.46	3.65	5.73	0.423	8	0.470	1.320	2.691	1.991
Zr	6.25	1.75	3.32	5.15	0.973	8	0.393	1.103	3.072	1.771
Tc	6.85	2.28	2.74	4.40	2.970	8	0.255	0.717	3.740	1.506
Ru	6.74	2.25	2.71	4.28	3.152	8	0.248	0.696	4.001	1.481
Hf	6.44	2.15	3.19	5.05	1.106	10	0.377	1.058	3.724	1.745
Re	8.03	2.68	2.76	4.46	3.715	10	0.246	0.691	4.409	1.520

Table 2: Values of y (=y_{min}) ,γ and z for 10 hcp metals.

Element	$y_{\min}$	$\gamma = (1+\frac{1}{\alpha\lambda})c_2 - 1$	$z \equiv n_{21} c_2^{p} e^{-\gamma y}$
Be	1.717	1.453	0.084
Mg	3.534	1.367	0.016
Sc	5.261	0.919	0.033
Ti	5.258	0.977	0.025
Y	6.906	0.836	0.028
Zr	6.889	0.863	0.024
Tc	6.937	0.953	0.011
Ru	6.914	0.944	0.013
Hf	8.518	0.792	0.021
Re	8.558	0.885	0.008

Table 3: Rigid and relaxed surface energies (in Jm^{-3}) of the (0001) surface of hcp metals

Element	Rigid	Relaxed		
		σ_T	σ_1	σ_2
Be	1.947	1.757	1.707	0.050
Mg	0.672	0.633	0.624	0.009
Sc	0.959	0.909	0.891	0.018
Ti	1.470	1.369	1.310	0.059
Y	0.810	0.766	0.761	0.005
Zr	1.388	1.305	1.291	0.014
Tc	2.619	2.455	2.398	0.057
Ru	2.384	2.186	2.123	0.063
Hf	1.573	1.500	1.476	0.024
Re	3.066	2.940	2.828	0.112

Table 4: Experimental and theoretical surface energies(in Jm^{-2}) for the (0001) surface of hcp metals.

Element	AECT(Present)	Semi-empirical calculations	First-principles calculations	Expt
Be	1.757	1.650[a]1.286[b]1.273[c]1.527[d]	2.122[e] 1.834[f]	2.700[g]
Mg	0.633	0.900[a] 0.310[c]0.289[d]	0.642[e] 0.792[f]	0.760[g]
Sc	0.909	1.355[a]0.706[c]0.816[d]	0.820[e] 1.834[f]	1.275[g]
Ti	1.369	1.962[a]1.824[b]1.033[c]1.402[d]	1.950[e] 2.632[f]	2.100[g]
Y	0.766	1.001[a]0.864[b]0.623[c]0.737[d]	0.680[e] 1.506[f]	1.125[g]
Zr	1.305	2.302[a]0.988[c]1.230[d]	1.530[e] 2.260[f]	2.000[g]
Tc	2.455	2.654[d]	2.800[e] 3.691[f]	3.150[g]
Ru	2.186	3.191[a]2.616[b]1.281[c]	3.320[e] 3.928[f]	3.050[g]
Hf	1.500	2.041[a]1.854[b]0.992[c]1.786[d]	1.750[e] 2.472[f]	2.150[g]
Re	2.940	3.940[a] 1.682[c]2.941[d]	3.270[e] 4.214[f]	3.600[g]

[a] Modified embedded atom method(MEAM) calculation, Ref.[39]
[b] Modified embedded atom method(MEAM) calculation, Ref.[40]
[c] Analytical modified embedded atom method(AMEAM) calculation, Ref.[41]
[d] Empirical electron theory (EET) calculations, Ref.[42]
[e] LMTO-ASA calculations, Ref.[37]
[f] FCD- GGA, Ref.[38]
[g] Experiment, Ref.[43]

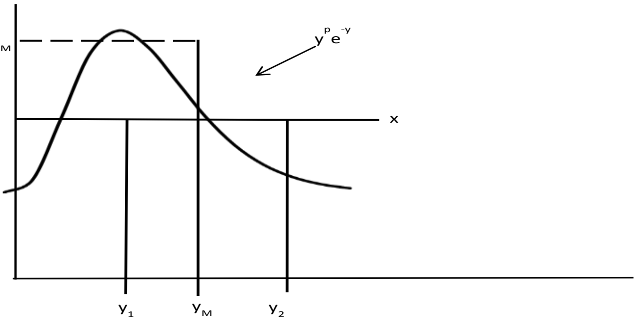

Fig. 1. Graphical illustration of Eq. (5) showing the appearance of two roots. The root y_1 is to the left of the maximum y_M that corresponds to a lattice parameter smaller than a_o ,while the root y_2 to the right of y_M corresponds to the lattice parameter larger than a_o .

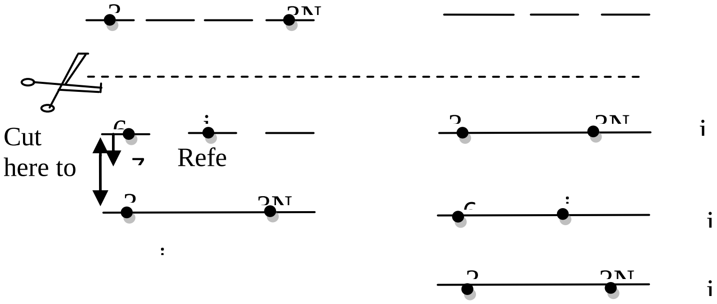

Fig.2.hcp (0001) planes after the creation of the surface, and the neighbour atoms in each plane to the reference atom i. The reference atom i is on the surface plane j = 1 in (i), while it is on the plane j = 2 in (ii). The planes indicated by dash lines are no longer there after the creation of the surface.

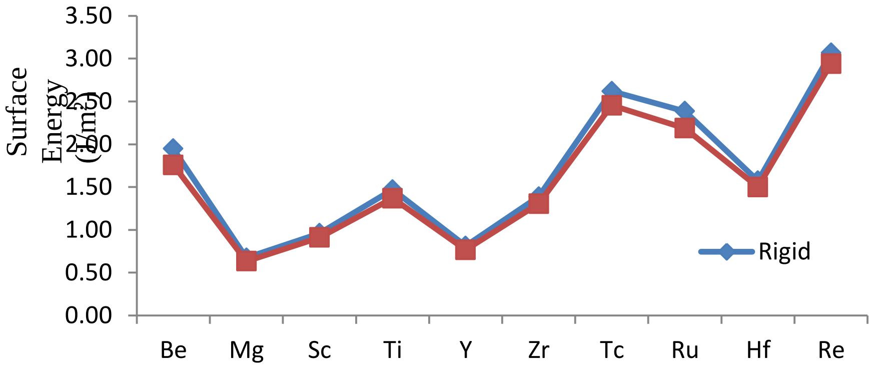

Fig.3. comparison of the rigid and relaxed AECT surface energies for the hcp (0001) surface for sp, 3d, 4d,and 5d metals. Solid diamond depicts rigid surface energy results and solid squares depict relaxed surface energy.

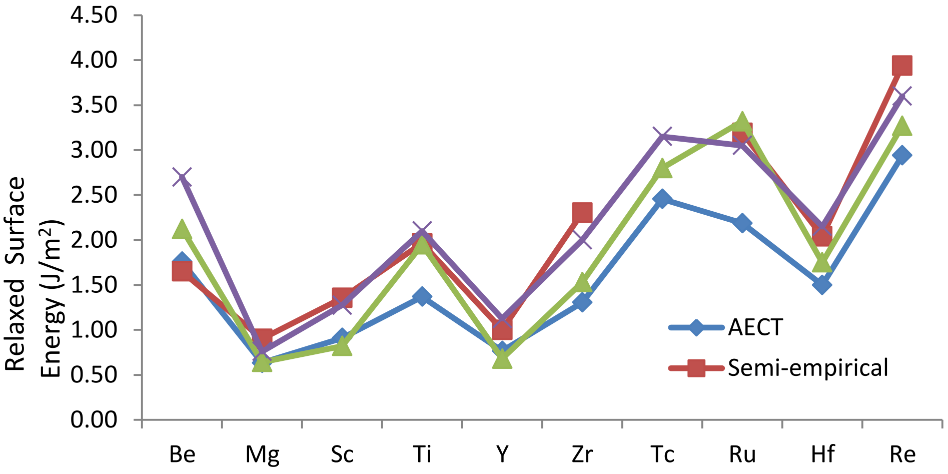

Fig.4. The calculated surface energies for the (0001) surfaces for sp, 3d, 4d and 5d metals. Solid diamond indicates results from AECT, compared to the structure independent surface energies derived from the surface tension of the liquid metals depicted by stars [43], ab initio calculations [37] depicted by solid triangle, and semi-empirical calculations [39] depicted by solid squares.

5.0 Conclusion

This study examined the effect of relaxation on the calculated surface energy for 10 hcp metals using the analytical equivalent crystal theory method. We have thus, successfully included the effect of relaxation for the first time to the surface energy results of the AECT method first proposed by Zypman and Ferrante [25] for fcc metals only. The decrease in the calculated surface energy values due to the effect of relaxation have been found to be of the orderof 4 - 10%.

The surface energies of the 10 hcp metals are in good agreement with the available first-principles calculations and experimental data. The results are also in reasonable agreement with the work of Baskes and Johnson [39]. Furthermore, the calculated surface energies for the 3d, 4d and 5d metals have been showed to exhibit the typical parabolic dependence on the d occupation as suggested by Friedel [44].

Acknowledgements

Fruitful discussions with Dr. S.O. Azi are gratefully acknowledged. E. Aghemenloh would like to thank the International centre for theoretical physics (ictp) for their ejds journal delivery assistance.

References

[1] J. Sokolov, F. Jona, P.M. Marcus, Solid State Commun. 49 (1984) 307.
[2] F. Jona, P.M. Marcus, in The structure of surfaces II, edited by J.F. Van der Veen, M. A. Van Hove, Springer series in surface sciences Vol. II (Springer – Verlag, Berlin, 1988), p. 90.
[3] N.D. Lang, W. Kohn, Phys. B1 (1970) 4555.
[4] M.W. Finnis, V. Heine, J. Phys. F (Met. Phys.) 4 (1974) L37
[5] G. Allan, M. Lannoo, Surf. Sci. 40 (1973) 375; Phys. Status Solidi (b) 74 (1976) 409; Phys. Rev. B37 (1988) 2678.
[6] R.N. Barnett, U. Landman, C.L. Cleveland, Phys. Rev. B 27 (1983) 6534.
[7] **R**.N. Barnett, U. Landman, C.L. Cleveland, Phys. Rev. Lett. 51 (1983) 1359
[8] P. Jiang, P.M. Marcus, F. Jona, Solid State Communi. 59 (9186) 275; Phys. Rev. B35 (1987) 7952.
[9] K.M. Ho, K.P. Bohnen, Phys. Rev. B32 (1985) 3446.
[10] C.L. Fu, S. Ohnishi, H. F. Jansen, A.J. Freemen, Phys. Rev. B 31 (1985) 1168.
[11] A. Eguiluz, Phys. Rev. B35 (1987) 5473.
[12] J.W. Davenport, M. Weinert, Phys. Rev. Lett. 58 (1987) 1382.
[13] D.R. Hamann, P.J. Feibelman, Phys. Rev. B 37 (1988) 3847.
[14] P.J. Feibelman, D.R. Hamann, Surf. Sci. 234 (1990) 377.
[15] M. Methfessel, D. Hennig, M. Scheffler, Phys. Rev. B 46 (1992) 4816.
[16] A. M. Rodriguez, G. Bozzolo, J. Ferrante, Surf. Sci. 289 (1993) 100.
[17] M.S. Daw, M.I. Baskes, Phys. Rev.Lett. 50 (1983) 1285.
[18] J.R. Smith, A. Banerjea, Phys. Rev. Lett. 59 (1987) 2451.

[19] J.R. Smith, A. Banerjea, Phys. Rev. B 37 (1988) 10411.
[20] J.R. Smith, T. Perry, A. Banerjea, J. Ferrante, G. Bozzolo, Phys. Rev. B 44 (1991) 6444.
[21] J. B. Adams, S.M. Foiles, Phys. Rev. B 41 (1990) 3316.
[22] T. Ning, Q.Yu, Y. Ye, Surf. Sci. 206 (1988) L857
[23] S.M. Foiles, M.I. Baskes, M.S. Daw, Phys. Rev. B 33 (1986) 7893
[24] S.P. Chen, D.J. Srolovitz, A. F. Voter, J. Mater. Res. 4 (1989) 62.
[25] F.R. Zypman, J,Ferrante, Comput. Mater. Sci. 42 (2008) 659.
[26] E. Aghemenloh, J.O.Umukoro, S.O. Azi, S. Yusuf, J.O.A. Idiodi, Comput. Mater. Sci. 50 (2011) 3290.
[27] E. Aghemenloh, S. Yusuf, J.O.A. Idiodi, Mater. Chem. Phys. 138 (2013) 529.
[28] J.R. Rose, J.R. Smith, J. FerrantePhys, Rev. B 28 (1983) 1835; J.R. Rose, J.R. Smith, F. Guinea, J. Ferrante, Phys. Rev. B 29 (1984) 2963.
[29] C. Kittle, Introduction to solid state physics, fifth ed. John Wiley and Sons, 1976. pp. 31-85.
[30] M. Igarashi. M. Khantha,V. Vitek, Philos. Mag. B 63 (1991) 603.
[31] R. C. Pasianot, E.J. Savino, Phys. Rev. B 45 (1992) 12704.
[32] D. H. Ruiz, L. M. Gribaudo, A. M. Monti, Zirconium and Hafnium. Computer simulation studies, Mater. Res. 8(4) (2005) 431.
[33] B. Hayes, Am. Sci. 93(2005) 104.
[34] F. Chapeau-Blondeau, A. Monir, Numerical evaluation of the Lambert W function and application to generation of generalized Gaussian noise with exponent ½, IEEE Trans. Signal Proc. 50 (2002) 2160
[35] E. Aghemenloh, J.O.A. Idiodi, S.O. Azi, Comput. Mater. Sci. 46 (2009) 524
[36] G. Bozzolo, J. Ferrante, A. M. Rodriguez, J. Comput-Aided. Mater. Design, 1(1993) 285.
[37] H.L.Skriver, N.M. Rosengaard, Phys. Rev. B 46 (1992) 7157.
[38] L.Vitos, A.V. Ruban, H.L. Skriver, J. Kollar, Surf. Sci. 411 (1998) 186.
[39] M.I. Baskes, R.A. Johnson, Modelling Simul. Mater. Sci. Eng. 2 (1994) 147.
[40] D.D. Wang, J.M. Zhang, K.W. Xu, Surf. Sci. 600 (2006) 2990.
[41] W.Hu, B. Zhang, B.Huang, F. Gao, D.J. Bacon, J. Phys. Condens. Matter. 13 (2001) 1193.
[42] B-Q, Fu, W. Liu, Z-L, Li, Applied Surf. Sci. 255 (2009) 9348.
[43] F.R. deBoer, R. Boom, W.C. M. Mattens, A. R. Miedema, A. K. Niessen, Cohesion inmetals (1988) North-Holland, Amsterdam.
[44] J. Friedel, Ann. Phys. 1(1976) 257